www.czasopisma.pan.pl PAN POLSKA AKADEMIA NAUK www.journals.pan.pl

Archives of Acoustics Vol. 49, No. 1, pp. 129–140 (2024), doi: 10.24425/aoa.2024.148771

Technical Note

Performance of the Direct Sequence Spread Spectrum Underwater Acoustic Communication System with Differential Detection in Strong Multipath Propagation Conditions

Jan H. SCHMIDT, Iwona KOCHAŃSKA*, Aleksander M. SCHMIDT

Faculty of Electronics, Telecommunication and Informatics, Department of Signals and Systems
Gdańsk University of Technology
Gdańsk, Poland

*Corresponding Author e-mail: iwona.kochanska@pg.edu.pl

(*received October 24, 2020; accepted April 2, 2020; published online January 8, 2024*)

The underwater acoustic communication (UAC) operating in very shallow-water should ensure reliable transmission in conditions of strong multipath propagation, significantly disturbing the received signal. One of the techniques to achieve this goal is the direct sequence spread spectrum (DSSS) technique, which consists in binary phase shift keying (BPSK) according to a pseudo-random spreading sequence.

This paper describes the DSSS data transmission tests in the simulation and experimental environment, using different types of pseudo-noise sequences: *m*-sequences and Kasami codes of the order 6 and 8. The transmitted signals are of different bandwidth and the detection at the receiver side was performed using two detection methods: non-differential and differential.

The performed experiments allowed to draw important conclusions for the designing of a physical layer of the shallow-water UAC system. Both, *m*-sequences and Kasami codes allow to achieve a similar bit error rate, which at best was less than 10^{-3}. At the same time, the 6th order sequences are not long enough to achieve an acceptable BER under strong multipath conditions. In the case of transmission of wideband signals the differential detection algorithm allows to achieve a significantly better BER (less than 10^{-2}) than non-differential one (BER not less than 10^{-1}). In the case of narrowband signals the simulation tests have shown that the non-differential algorithm gives a better BER, but experimental tests under conditions of strong multipath propagation did not confirm it. The differential algorithm allowed to achieve a BER less than 10^{-2} in experimental tests, while the second algorithm allowed to obtain, at best, a BER less than 10^{-1}. In addition, two indicators have been proposed for a rough assessment which of the detection algorithms under current propagation conditions in the channel will allow to obtain a better BER.

Keywords: direct sequence spread spectrum; DSSS, *m*-sequences; Kasami codes; shallow-water channel; multipath propagation; underwater acoustic communications; UAC.

Copyright © 2024 The Author(s).
This work is licensed under the Creative Commons Attribution 4.0 International CC BY 4.0 (https://creativecommons.org/licenses/by/4.0/).

1. Introduction

The underwater acoustic communication (UAC) system should efficiently use the UAC channel bandwidth to perform the reliable data transmission. To achieve this goal spread spectrum techniques can be used in the physical layer of data transmission (Schmidt, 2020). One of them is the direct sequence spread spectrum (DSSS) technique. Its advantage is the fact that the knowledge of the pseudo-random sequence on the receiving side is required for correct receipt of information. Keeping this sequence secret may be part of the protection against unauthorised access to transmitted information. Pseudorandom spreading sequences used in DSSS systems should be characterized by a normalized autocorrelation function as close as possible to the Kronecker delta. For this reason, in telecommunications systems with the spread spectrum technique, the maximum length sequences (*m*-sequences) are used (Zepernick, Finger, 2005). In systems using the code multiple access technique, the spreading sequences used should also have as lit-

tle cross-correlation as possible. Both these requirements are met by Kasami sequences (Sarwate, Pursley, 1980).

Descriptions of numerous implementations of the DSSS technique in underwater telecommunications systems can be found in the literature. Some of them, similar to radiocommunication systems, implement the RAKE algorithm in the receiver. However, this is not the only way to receive DSSS signals in UAC systems. Many of them implement matched filtration instead of the RAKE technique (Freitag, Stojanovic, 2004; Freitag *et al.*, 2001; Mironov *et al.*, 2018). Among these systems, few operate in shallow waters (Pelekanakis, Cazzanti, 2018; Qu *et al.*, 2018; Ra *et al.*, 2021; Freitag *et al.*, 2001; Sozer *et al.*, 1999). These are systems operating in different frequency bands, using m-sequences, Kasami sequences or Gold sequences – also of different ranks. Moreover, each of these systems was tested in different conditions.

In (Kochanska *et al.*, 2021) the results of DSSS signal transmission experiments aimed at comparing the possible data transmission rate with the use of different pseudorandom spreading sequences and depending on the bandwidth of the UAC system were described. A filtering method has been implemented in the receiver to detect information. The analysis of the results has shown that in conditions of strong multipath propagation, the BER of the transmission of signals of narrower bandwidth is better, than in the case of wider transmission bandwidth. Moreover, using m-sequences allowed to obtain better BER than the use of other PN sequences.

In (Kochańska, 2021) a new algorithm of differential detection of the DSSS signal, constructed of m-sequences of rank 8, has been described. The simulation and experimental tests have shown that this detection technique allows to obtain better values of BER than the algorithm applied in the system using this particular DSSS signals, described in (Kochanska *et al.*, 2021), but only for the transmission of wideband signals.

As mentioned in (Kochanska *et al.*, 2021), the DSSS-based UAC systems described in the literature use specific PN sequences and the fixed transmission bandwidth. To the best of the authors' knowledge, there are no publications presenting an analysis of the underwater DSSS system's performance depending on its bandwidth or the PN sequence used.

In this paper a comparison of the performance of two detection techniques is presented, applied in a laboratory model of the UAC system using a wide set of DSSS signals: constructed using m-sequences and Kasami codes of rank 6 and 8, occupying five different bandwidths from 1 to 5 kHz. The shallow-water channel was simulated using the Watermark simulator (van Walree, 2011), and the experimental tests were performed in the model pool.

2. Structure of communication signal

The process of the DSS signal generation is shown in Fig. 1. The input data stream $d[n]$ is converted into binary phase-shift keying (BPSK) symbols which are multiplied by the PN sequence $m[n]$ and the result is upsampled by the factor $R = \frac{f_s}{B}$ equal to the quotient of sampling frequency f_s (which is 200 kHz) and the system bandwidth B. The upsampled signal $x[n]$ is then used for phase modulation of the digital carrier waveform of the frequency f_c.

Two types of PN sequences are used for DSSS signal generation, namely m-sequences and Kasami codes of rank 6 and 8. Its autocorrelation functions are shown in Figs. 2 and 3.

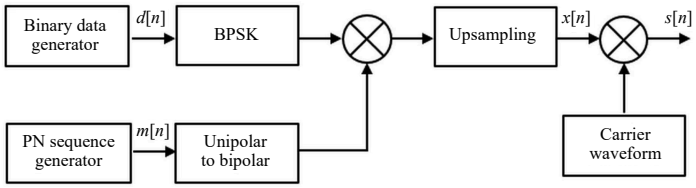

Fig. 1. Generation of the DSSS signal.

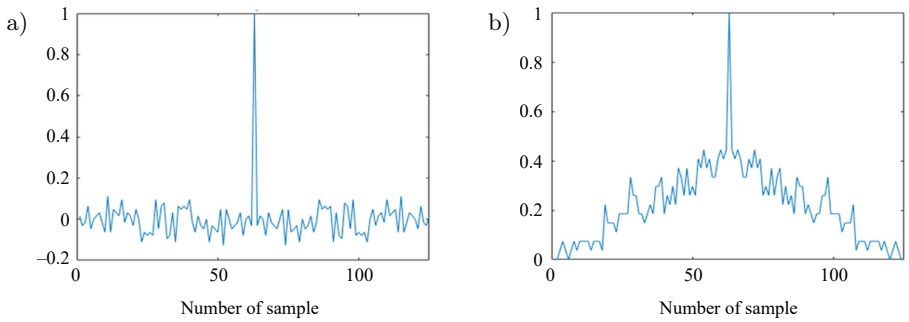

Fig. 2. Autocorrelation functions of PN sequences of rank 6: m-sequence (a) and Kasami code (b).

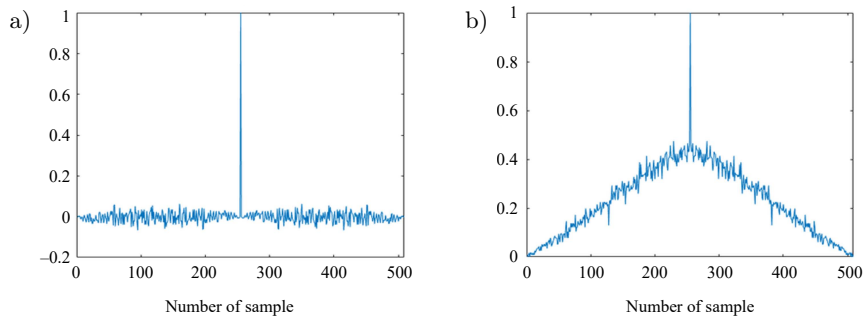

Fig. 3. Autocorrelation functions of PN sequences of rank 8: m-sequence (a) and Kasami code (b).

Table 1. DSSS signal parameters.

Bandwidth B [kHz]	Upsampling factor R	PN sequences rank	Symbol length N_s	Symbol duration T_s [ms]	Transmission rate [bps]
1	200	6	12600	63.00	15.87
1	200	8	51000	255.00	3.92
2	100	6	6300	31.50	31.75
2	100	8	25500	127.50	7.84
4	50	6	3150	15.75	63.49
4	50	8	12750	63.75	15.69
5	40	6	2520	12.60	79.37
5	40	8	10200	51.00	19.61

The generated signals occupy different bandwidths B, as shown in Table 1. The bandwidth B determines the upsampling factor R. The upsampling factor and the number of samples of PN sequence (which depends on its rank) determine the length of a single DSSS symbol N_s, as well as its duration T_s for a given sampling frequency f_c = 200 kHz The transmission rate has been calculated as a number of symbols per second.

3. The DSSS demodulator

At the receiver side (Fig. 4), the baseband equivalent signal $y_b[n]$ is calculated based on $y[n]$ and filtered by a matched filter described by complex-value coefficients $m_c[n] = m[n] + j\widehat{m}[n]$, where $m[n]$ is the PN sequence used for construction of a transmitted signal, and $\widehat{m}[n]$ is equal to the Hilbert transform of $m[n]$. Next the output of the matched filter is processed by the detection algorithms.

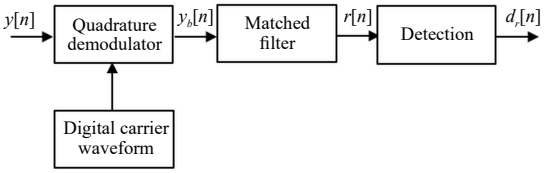

Fig. 4. Digital processing path of DSSS signal at the receiver side.

3.1. Detection algorithm A

The differential algorithm A has been described previously in (Kochańska, 2021). It is based on the assumption that the influence of the propagation conditions on the transmitted adjacent modulation symbols is similar. Therefore, in quasi-stationary conditions the response of the matched filter to subsequent modulation symbols is similar. If adjacent modulation symbols carry different information, then the modulus of the matched filter responses for these symbols is almost the same, while the phase will be opposite.

The output $r[n]$ of the matched filter is divided to segments of the length N_s (Table 1). For every two subsequent segments r_{k-1} and r_k of the signal $r[n]$ the Pearson correlation coefficient $C[k]$ of its arguments is calculated as:

$$C[k] = \frac{1}{L-1}\sum_{i=1}^{L}\frac{(\arg r_k[i] - \mu_k)}{\sigma_k}\frac{(\arg r_{k-1}[i] - \mu_{k-1})}{\sigma_{k-1}}, \tag{1}$$

where μ_k and μ_{k-1} are the mean values, and σ_k and σ_{k-1} are standard deviations of arguments of segments r_k and r_{k-1}, respectively.

If the value of the correlation coefficient $C[k]$ is positive or equal to 0, it indicates that a given segment of $r[n]$ represents the same information as the previous one. A negative value of $C[k]$ means that the information bit is the negation of the previous one. It can be expressed as:

$$d_r[k] = \begin{cases} d_r[k-1] & \text{if} \quad C[k] \geq 0, \\ \sim d_r[k-1] & \text{if} \quad C[k] < 0, \end{cases} \tag{2}$$

where k is the index of information bit number, corresponding to a given segment of $r[n]$.

The construction of this algorithm is such that its performance should increase when the similarity between amplitudes of consecutive DSSS symbols at the matched filter output increases. With a large similarity of amplitude, the only significant difference is the phase of these symbols, which is the transmitted information. To confirm this thesis for all received symbols a mean value C_A of the absolute values of the correlation coefficient $C[k]$ has been calculated:

$$C_A = \frac{1}{K}\sum_{k=1}^{K}|C[k]|, \tag{3}$$

which can be related to BER achieved with the algorithm A during simulation and experimental tests.

3.2. Detection algorithm B

The second detection algorithm B was applied during the simulation and experimental tests described in (Kochanska *et al.*, 2021). It compares the minimum $A_{\min}[k]$ and maximum $A_{\max}[k]$ values of the real part of the matched filter output $r[n]$. If the maximum value $A_{\max}[k]$ is greater than the absolute value $A_{\min}[k]$ then the modulation symbol carries a bit information equal to 1, otherwise the information is equal to 0. It can be denoted as:

$$d_r[k] = \begin{cases} 1 & \text{if} \quad A_{\max}[k] \geq |A_{\min}[k]|, \\ 0 & \text{if} \quad A_{\max}[k] < |A_{\min}[k]|. \end{cases} \tag{4}$$

The algorithm can perform effectively if the communication channel is characterized by a stable dominant propagation path well separated from the other paths. Then, also in the waveform at the output of the matched filter, a stable, dominant extreme "peak" will be observed, which is detected by the algorithm B as the $A_{\max}$ or $A_{\min}$ value. In order to make it possible to confirm this thesis, the coefficient C_B was defined:

$$C_B = \frac{C_{\text{ex}}}{C_{\text{all}}}, \tag{5}$$

where C_{ex} is the number of received DSSS symbols, in which at the output of the matched filter the extreme appeares for the most frequant delay among all symbols, and C_{all} is the number of all received symbols. It is expected, that the higher C_{ex} to C_{all} ratio is, the better BER should be obtained with the use of the algorithm B.

4. Simulation tests

The performance of the DSSS-based UAC system has been tested using the Watermark simulator for MATLAB software environment. It is a replay channel using at-sea measurements of time-varying impulse responses of UAC channels (van Walree, 2011), valued in the hydroacoustic environment. Three channels available at Watermark and representing different propagation conditions were selected, namely: Norway-Oslofjord (NOF1), Norway-Continental Shelf (NCS1), and Brest Commercial Harbor (BCH1).

NOF1 is a channel measured in a shallow stretch of Oslofjorden between a stationary source and a stationary single-hydrophone receiver. It represents a relatively smooth communication channel. The first arrival path, as shown in Fig. 5 presenting the scattering function of the channel, has no frequency spread, whereas later arrivals are Doppler spreads due to sea surface interactions. Most energy of the received signal is concentrated in a narrow delay-Doppler window.

NCS1 was measured similarly as NOF1, between a stationary source and a stationary single-hydrophone receiver. The measurements were conducted on Norway's continental shelf. As shown in Fig. 6, most energy is also concentrated at the start of the impulse response, but considering the next arrival paths, the differences from NOF1 are significant. There are no stable paths, thus it is more challenging than NOF1, in particular for coherent communication schemes such as DSSS, which need to detect the phase of a signal.

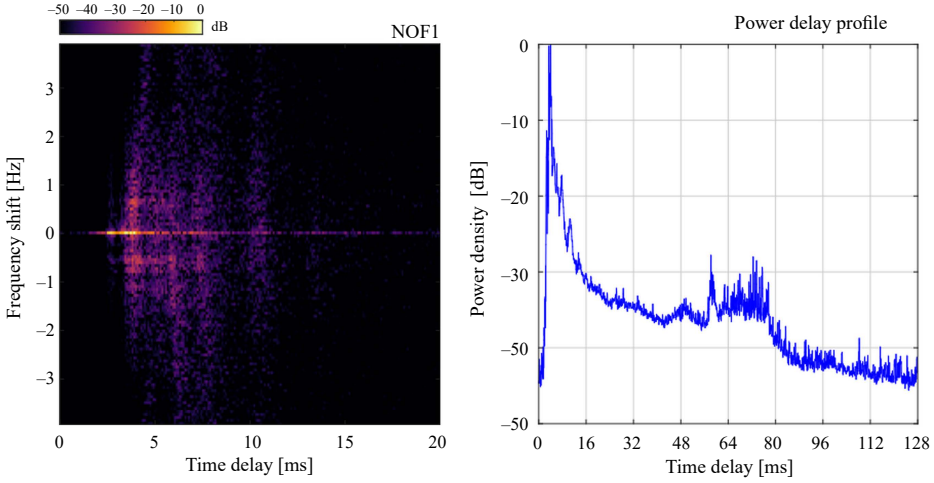

Fig. 5. Scattering function and power delay profile of NOF1 channel (van Walree, 2011).

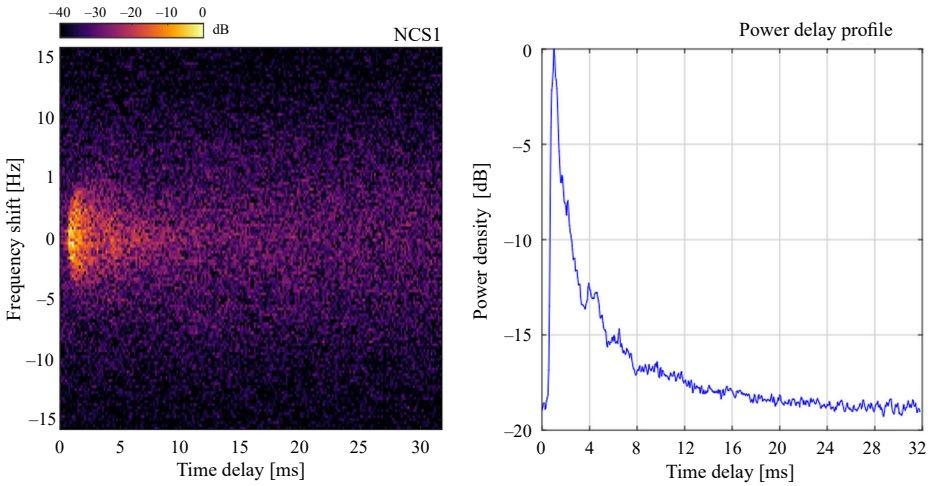

Fig. 6. Scattering function (a) and power delay profile (b) of NCS1 channel (VAN WALREE, 2011).

BCH1 channel was measured in the harbour of Brest, France. A source and a receiver were not stationary mounted at the bottom, as in case of NOF1 and NCS1, but lowered into the water column from two docks. Similarly to NOF1, the channel is a mixture of stable and fluctuating arrivals, but with a larger number of distinct trailing paths (Fig. 7) (VAN WALREE, 2011).

These three channels, representing different propagation conditions, were used to simulate the DSSS signal transmission.

During the simulation tests, different carrier frequencies were used to fit the DSSS signal to the frequency band of a given Watermark channel. It was equal to 14 kHz in case of NOF1 and NCS1 channels and 35 kHz in case of BCH1 channel.

As described in Sec. 2, 16 kinds of DSSS signals were transmitted in each of Watermark channels. They differed in kind of the PN spreading sequence, its length, and the bandwidth. Using each of the three Watermark channels, 180 transmission tests were performed using every DSSS signal of time duration equal to 6 s. Every DSSS signal was carrying different information bits. The detection of information was performed using the detection algorithm A and B.

Figure 8 shows the exemplary real part of the filter output of the matched DSSS receiver in the case of receiving a DSSS signal (constructed of m-sequence of rank 8) with a bandwidth of 1 kHz, representing the "0" bit value and the "1" bit value on the NOF1 channel. The extreme of the waveform occurs in the same place, with a different sign for the "0" and "1" bits. Figure 9 shows the real part of the response of the matched filter to a signal with a bandwidth of 4 kHz, carrying the value of the "0" bit and the value of the "1" bit. It can be seen that in case of wideband signal transmitted in stationary NOF1 channel the dominant path might not occur in the output waveform of the filter with the same delay.

The results of a bit error rate (BER) achieved in all 180 transmission tests of each DSSS signal are shown in Figs. 10, 12, 14, and 16. In Figs. 11, 13, 15, and 17 the coefficients C_A and C_B also calculated for all transmission tests are presented.

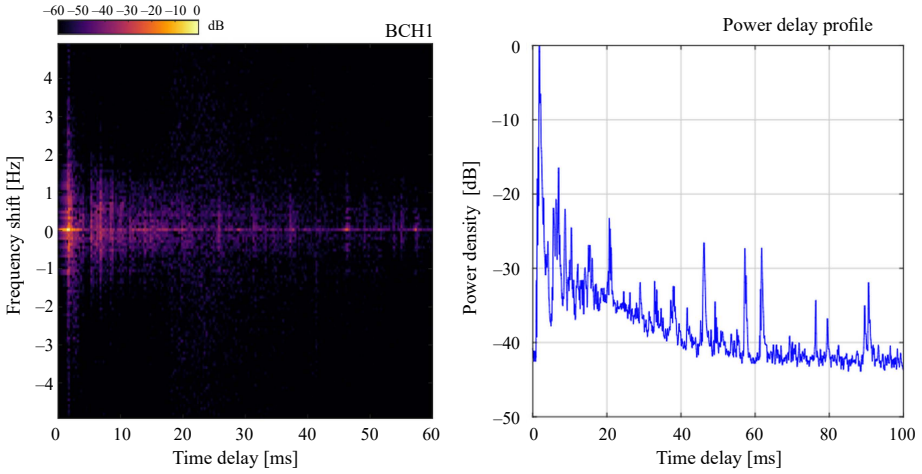

Fig. 7. Scattering function and power delay profile of BCH1 channel (VAN WALREE, 2011).

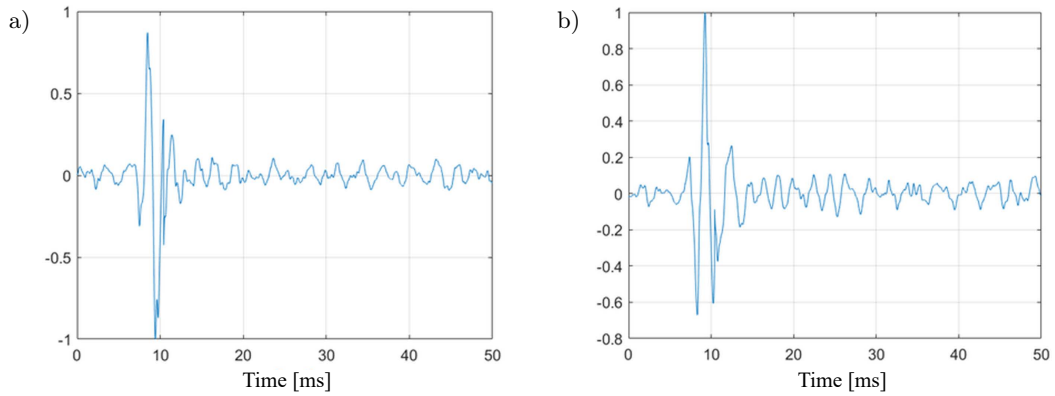

Fig. 8. Real part of the response of matched filter to DSSS signal constructed of m-sequence of rank 8 and bandwidth equal to 1 kHz, received in NOF1 channel, representing the "0" bit value (a) and the "1" bit value (b).

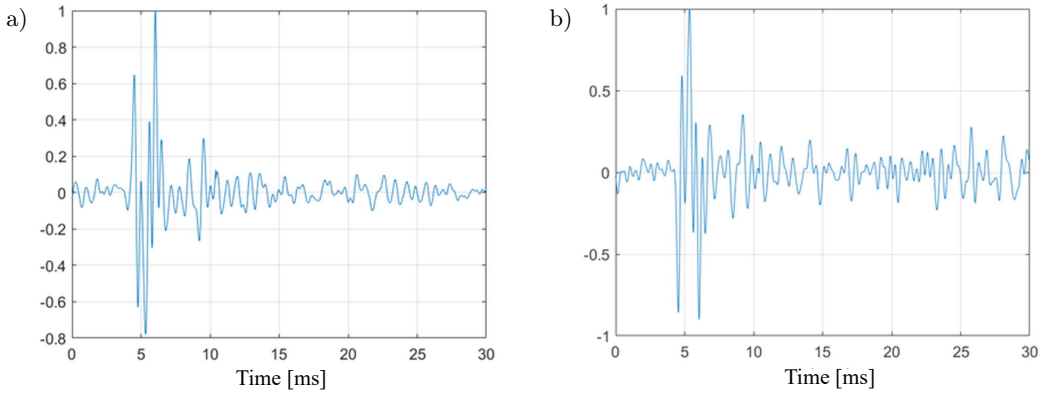

Fig. 9. Real part of the response of matched filter to DSSS signal constructed of m-sequence of rank 8 and bandwidth equal to 4 kHz, received in NOF1 channel, representing the "0" bit value (a) and the "1" bit value (b).

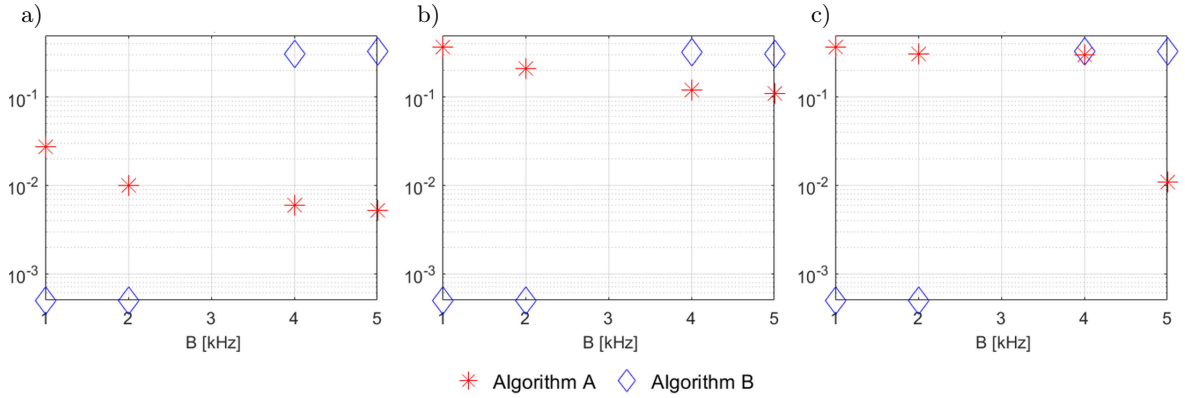

Fig. 10. The BER of the simulated transmission using DSSS signals constructed of m-sequences of rank 8 in NOF1 (a), NCS1 (b), and BCH1 (c) watermark channel.

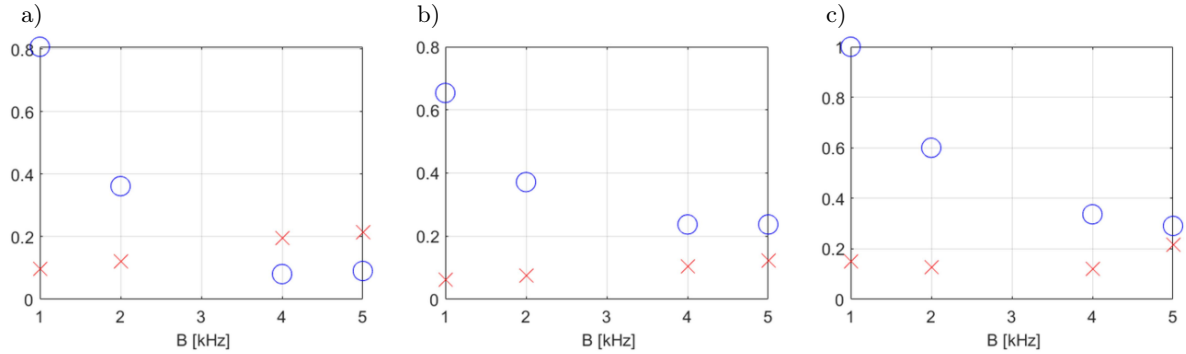

Fig. 11. The coefficients: C_A (×) and C_B (○) for transmission of DSSS signals constructed of m-sequnces of rank 8 in NOF1 (a), NCS1 (b), and BCH1 (c) watermark channel.

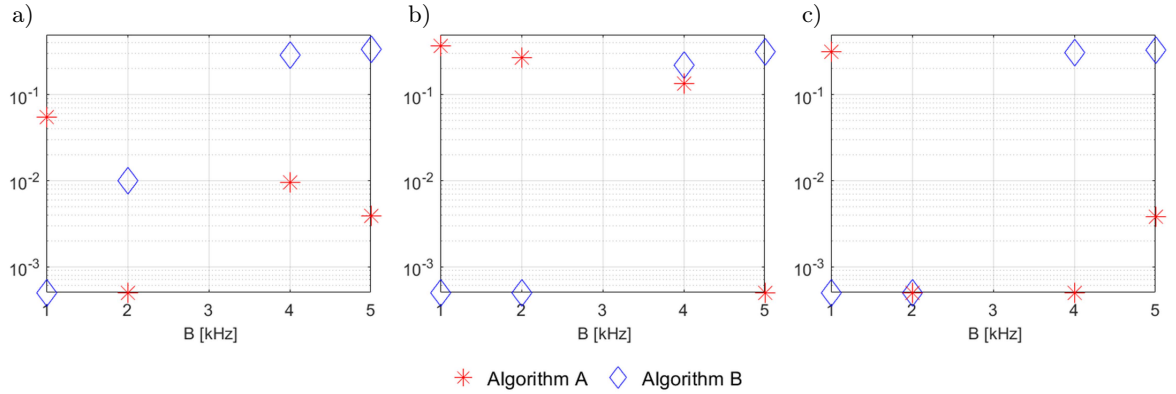

Fig. 12. The BER of the simulated transmission using DSSS signals constructed of Kasami of rank 8 in NOF1 (a), NCS1 (b), and BCH1 (c) watermark channel.

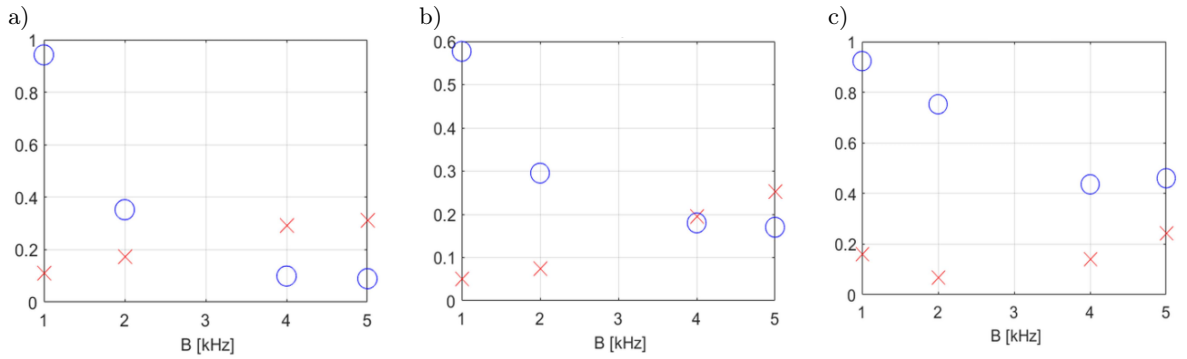

Fig. 13. The coefficients: C_A (×) and C_B (○) for transmission of DSSS signals constructed of Kasami codes of rank 8 in NOF1 (a), NCS1 (b), and BCH1 (c) watermark channel.

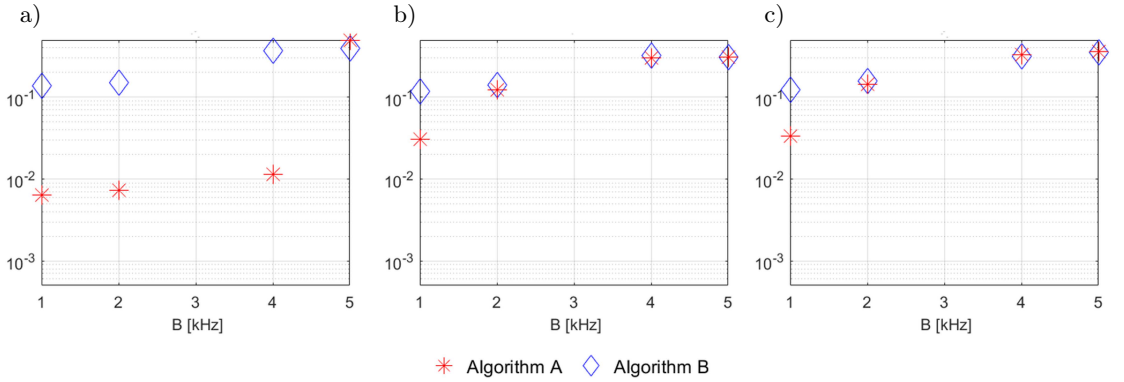

Fig. 14. The BER of the simulated transmission using DSSS signals constructed of m-sequences of rank 6 in NOF1 (a), NCS1 (b), and BCH1 (c) Watermark channel.

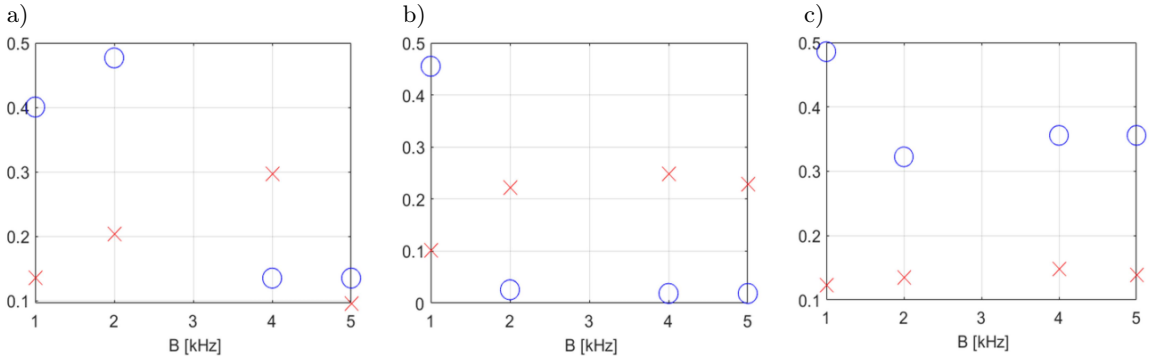

Fig. 15. The coefficients: C_A (×) and C_B (○) for transmission of DSSS signals constructed of m-sequnces of rank 6 in NOF1 (a), NCS1 (b), and BCH1 (c) Watermark channel.

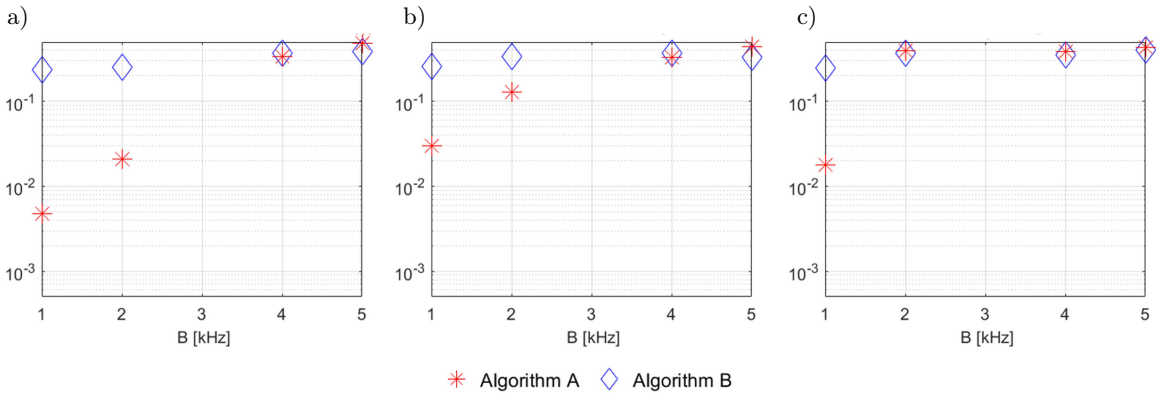

Fig. 16. The BER of the simulated transmission using DSSS signals constructed of Kasami codes of rank 6 in NOF1 (a), NCS1 (b), and BCH1 (c) Watermark channel.

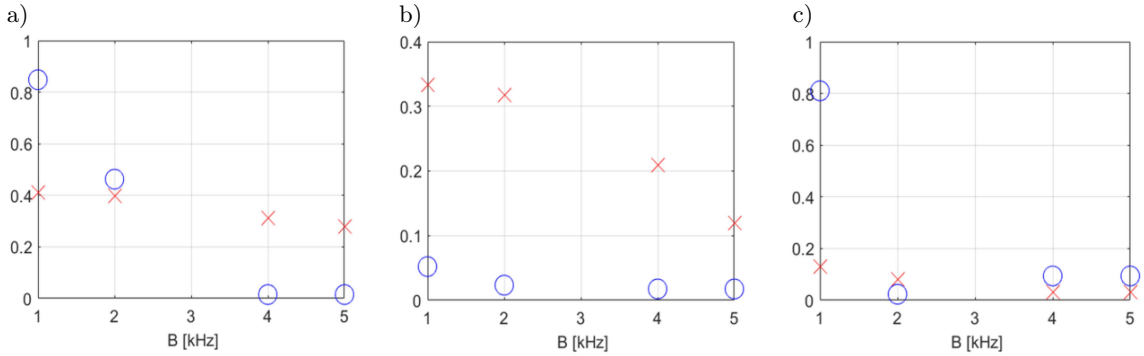

Fig. 17. The coefficients: C_A (×) and C_B (○) for transmission of DSSS signals constructed of Kasami codes of rank 6 in NOF1 (a), NCS1 (b), and BCH1 (c) Watermark channel.

During simulation tests with the use of m-sequences of the order 8, the use of the algorithm B allowed to obtain a BER less than 10^{-3} in each of the tested channels in the case of a bandwidth equal to 1 and 2 kHz. The use of the algorithm A gave much worse results (BER $<10^{-1}$ in the NOF1 channel and BER $>10^{-1}$ in the NCS1 and BCH1 channels). However, in wider frequency bands (4 and 5 kHz) it was the algorithm A that produced a lower BER than the algorithm B.

Using Kasami codes of the rank 8, a BER less than 10^{-3} was obtained with the detection algorithm B for a bandwidth of 1 kHz (a BER was less than 10^{-1} with the algorithm A) and the width detection algorithm A for a bandwidth of 2 kHz (a BER was of the rank 10^{-1} with the algorithm B). For a bandwidth equal to 4 and 5 kHz, the algorithm A made it possible to obtain a BER of the rank 10^{-2}, while the algorithm B produced a BER greater than 10^{-1}. In NCS1 and BCH1 channels the algorithm B made it possible to obtain a BER less than 10^{-3} for bandwidths of 1 and 2 kHz, while the algorithm A gave a BER greater than 10^{-1} in both bands in the NCS1 channel, and a BER greater than 10^{-1} for the 1 kHz bandwidth and a BER less than 10^{-3} for a bandwidth equal to 2 kHz. When detecting a signal with a bandwidth of 4 and 5 kHz the algorithm A turned out to give better results than the algorithm B.

Thus, using signals constructed of PN sequences of the rank 8 in each of the tested channels, it was observed that the algorithm A gives better results in case of 4 and 5 kHz bandwidth signals, while for signals of a bandwidth equal to 1 and 2 kHz, the algorithm B makes possible to achieve a better BER than the algorithm A.

Analysis of the value of the C_B coefficient (Fig. 11), determining "how often" the extremum at the output of the matched filter has the same delay, allows to confirm that with an increase of the signal bandwidth, the value of this coefficient decreases, and thus decreases the stability of the "peak" delay on the output of the matched filter, which is recognized as an extremum. In turn, the comparison of the BER graphs obtained for the B algorithm and the C_B coefficient values confirms the thesis that a decrease in the C_B coefficient is accompanied by the deterioration of the BER obtained using the B algorithm.

The relationship between the BER obtained by the algorithm A and the coefficient C_A is less clear than in the case of the algorithm B and the coefficient C_B. The value of the C_A coefficient obtained during all tests using sequences of the order 8 oscillates around the value of 0.2. However, as can be seen in the BER plots in Fig. 10 and 12, such a small average value of the absolute value of the correlation coefficient between

successive symbols at the output of the matched filter is sufficient for the detection algorithm A to work with a BER of even 10^{-3}, so it made an incorrect decision less than once every 1000 symbols based on the value of the correlation coefficient between adjacent symbols at the matched filter output.

During tests conducted using DSSS signals built from m-sequences of the rank 6 (Fig. 14), it was possible to obtain a BER of the rank of 10^{-2} only in NOF1 using the detection algorithm A. For a bandwidth equal to 5 kHz band, the BER obtained with both detection methods was greater than 10^{-1}. The use of Kasami codes of a length 6 gave a BER of the rank 10^{-2} for the 1 and 2 kHz bandwidths using the algorithm A, also in the NOF1 channel. In case of other two channels detection algorithms failed to achieve a BER less than 10^{-2}.

In contrast to the results of tests carried out for signals constructed from sequences of the rank 8, in the case of signals built on sequences of the 6th order, i.e., 4 times shorter, it is difficult to observe the relationship between a BER and the C_A and C_B coefficients. Although the C_B coefficient in most tests has much higher values in the 1 kHz bandwidth than in the other bands, the BER obtained in this band using the B algorithm is not lower than 10^{-1} and at the same time close to the BER obtained with the same algorithm in the other bands.

5. Experimental tests

Experimental tests of DSSS communication were carried out in the model pool of the Gdańsk University of Technology. The pool is 40 m long, 4 m wide, and 3 m deep. During the experiment the transmitting and receiving transducers were immersed to a depth of 1.5 m (Schmidt, Schmidt, 2023). On both, transmitter and receiver sides, the laboratory model of the UAC system consisted of laptop computers with the MATLAB environment, underwater HTL-10 telephones (Schmidt, 2016), NI-USB6363 recording and generating devices and omnidirectional transducers with a resonant frequency of 34 kHz. A more detailed description of the experiment setup can be found in (Kochanska *et al.*, 2021).

5.1. Channel characteristics

The communication tests were preceded by measurements of the time-varying impulse responses (TVIR) of the UAC using correlation method and pseudo-random binary sequence (PRBS) probe signals, constructed of m-sequence of the rank 8. The probe signals were of four different bandwidths: 1, 2, 4, and 5 kHz, and the carrier frequency was equal to 30 kHz. The sampling frequency on the receiving side was equal to 200 kHz. Figure 18 shows modules of TVIRs measured using signals of a bandwidth equal to 1 and 5 kHz.

5.2. Communication tests

Similarly as in simulation tests, 16 kinds of DSSS signals were transmitted in the communication channel in a model pool. The carrier frequency of each signal was equal to 30 kHz. Every DSSS signal carried different information bits. The detection of information was performed using both detection algorithms – A and B. The results of achieved BER are shown in Figs. 19 and 21. Figures 20 and 22 show corresponding values of the coefficients C_A and C_B.

During transmission tests of signals constructed of PN sequences of the rank 6, a BER less than 10^{-3} was achieved in the 1 kHz bandwidth using the detection algorithm A. For the 2 kHz bandwidth, such a BER was obtained only in the case of the Kasami codes. The detection algorithm B did not allow to obtain a BER less than 10^{-1} in any of the transmission bands, even though the C_B coefficient was relatively high in some bands. Similarly, in the case of the use of pseudorandom sequences of the rank 8, the algorithm B did not allow to obtain a BER less than 10^{-1} (except for the 2 kHz bandwidth in the case of Kasami code). On the other hand, using the algorithm A allowed to obtain BER less than 10^{-3} in most transmission tests. The worst result was a BER less 10^{-2}

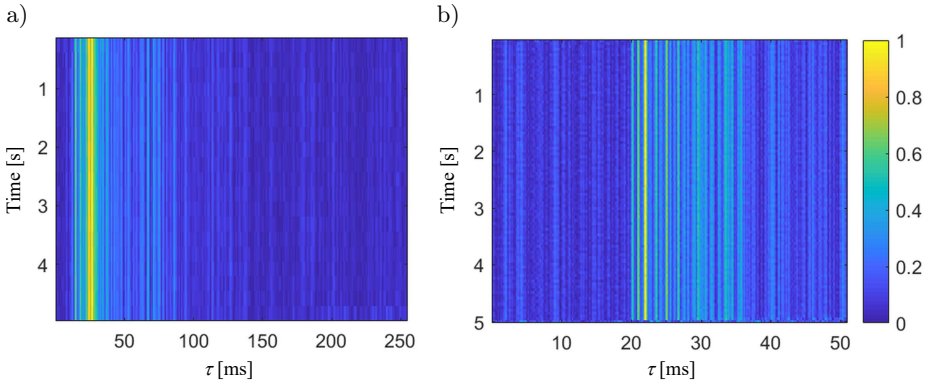

Fig. 18. Modules of TVIRs measured in the model pool using signals of bandwidth equal to 1 kHz (a) and 5 kHz (b).

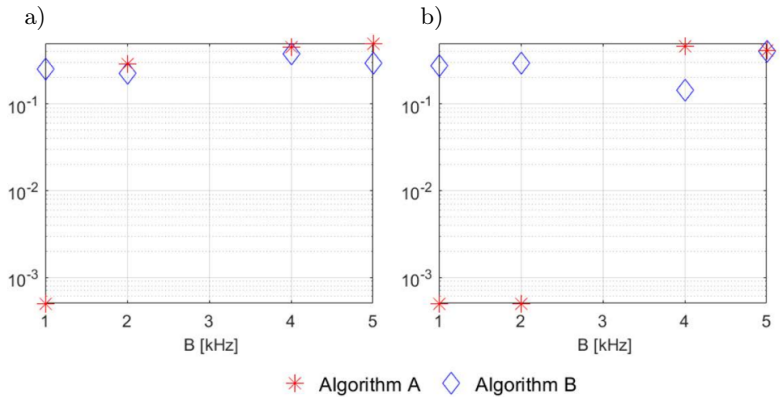

Fig. 19. The BER of the data transmission in model pool using DSSS signals constructed of m-sequences (a) and Kasami codes (b) of rank 6.

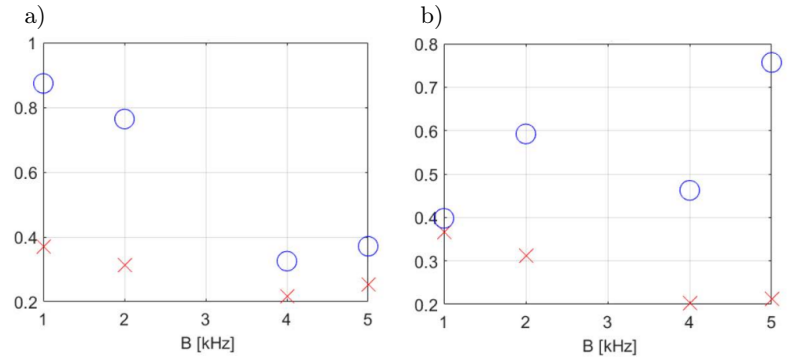

Fig. 20. The coefficients: C_A (×) and C_B (○) for transmission in model pool of DSSS signals constructed of m-sequences (a) and Kasami codes (b) of rank 6.

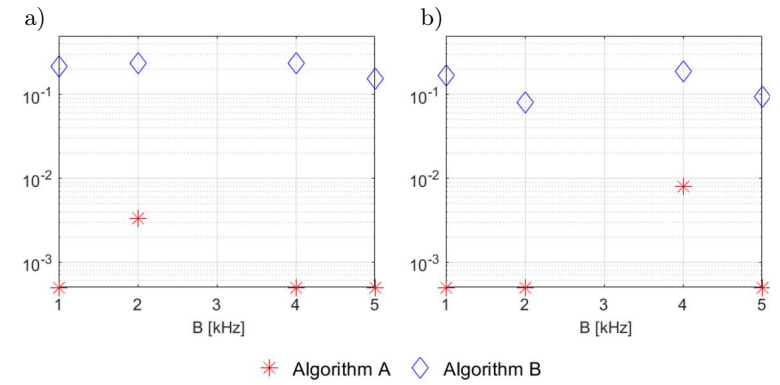

Fig. 21. The BER of the data transmission in model pool using DSSS signals constructed of m-sequences (a) and Kasami codes (b) of rank 8.

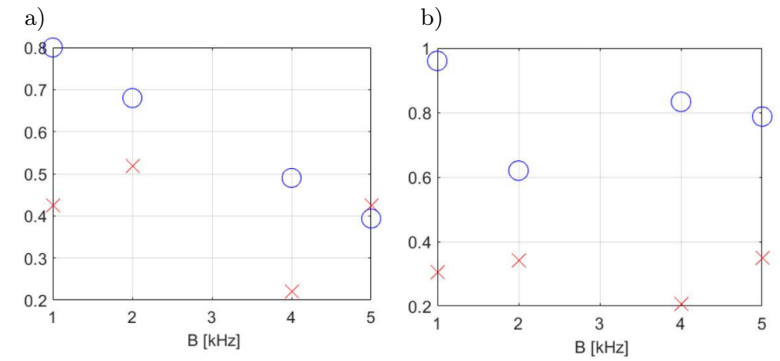

Fig. 22. The coefficients: C_A (×) and C_B (○) for transmission in model pool of DSSS signals constructed of m-sequnces (a) and Kasami codes (b) of rank 8.

for the 2 kHz bandwidth in the case of m-sequences and for the 4 kHz bandwidth in the case of Kasami sequences. Both for Kasami codes of the rank 6 and for the rank 8, a relationship was observed between an increase in the value of the C_A coefficient and the improvement in a BER obtained using the A algorithm. In the case of m-sequences, no such relationship was observed.

6. Conclusions

The simulation tests conducted with the use of three different simulation models of the UAC channel in a multipath environment and experimental tests conducted in a model pool allowed the formulation of the following conclusions, which are important guidelines for the design of the physical layer of the UAC DSSS system operating in very shallow waters.

The use of m-sequences and Kasami codes as spreading sequences allows to obtain a similar BER, so there are no contraindications to use Kasami sequences in systems with the code multiple access technique due to their good cross-correlation properties.

The order of 8 sequences allowed to obtain a much better BER than the order of 6 sequences. In a UAC system operating in very shallow waters, the longer ones should be used, at the expense of the achievable transmission rate.

The simulation studies carried out confirmed the thesis mentioned earlier in the article (Kochańska, 2021) that the detection algorithm A will allow to obtain a better BER than the detection algorithm B in the case of transmission in a wider band, i.e., 4 and 5 kHz. The algorithm B, on the other hand, performs better in narrower bands: 1 and 2 kHz. However, during experimental tests in the model pool, where multipath propagation was particularly strong, only the algorithm A (in each transmission band) allowed to obtain an acceptable BER.

Two indicators presented in the article: the C_A coefficient, assessing the degree of similarity of successive DSSS symbols at the output of the matched receiver, and the C_B coefficient, evaluating the delay stability of the dominant propagation path in the channel, are helpful in interpreting the differences in the transmission BER obtained by the two tested detection algorithms and can be used to predict which of the detection algorithms, under current propagation conditions in the channel, will allow to obtain a better BER. However, the relationship between the BER obtained by the B algorithm and the C_B index was much more clearly visible in the studies using the 8th order sequence than the relationship between the index C_A and a BER obtained with the algorithm A. These indicators can be used in the adaptive UAC system, enabling a rough assessment of the current conditions in the channel and, depending on them, the selection of a detection algorithm for the current operation in the receiver.

Acknowledgments

The paper was written as a result of the research project no. DOB-SZAFIR/01/B/017/04/2021 financed by the National Centre for Research and Development.

References

1. Freitag L., Stojanovic M. (2004), MMSE acquisition of DSSS acoustic communications signals, [in:] *Oceans '04 MTS/IEEE Techno-Ocean '04*, pp. 14–19, doi: 10.1109/OCEANS.2004.1402888.
2. Freitag L., Stojanovic M., Singh S., Johnson M. (2001), Analysis of channel effects on direct-sequence and frequency-hopped spread-spectrum acoustic communication, *IEEE Journal of Oceanic Engineering*, **26**: 586–593, doi: 10.1109/48.972098.
3. Kochańska I. (2021), A new direct-sequence spread spectrum signal detection method for underwater acoustic communications in shallow-water channel, *Vibrations in Physical Systems,* **32**(1): 2021106, doi: 10.21008/j.0860-6897.2021.1.06.
4. Kochanska I., Salamon R., Schmidt J., Schmidt A. (2021), Study of the performance of DSSS UAC system depending on the system bandwidth and the spreading sequence, *Sensors*, **21**: 2484, doi: 10.3390/s21072484.
5. Mironov A.S., Burdinskiy I.N., Karabanov I.V. (2018), The method of defining the threshold value of the symbolic correlation function for detecting DSSS hydroacoustic signal, *2018 International Multi-Conference on Industrial Engineering and Modern Technologies (FarEastCon)*, pp. 1–6, doi: 10.1109/FarEastCon.2018.8602588.
6. Pelekanakis K., Cazzanti L. (2018), On adaptive modulation for low SNR underwater acoustic communications, *OCEANS 2018 MTS/IEEE*, pp. 1–6, doi: 10.1109/OCEANS.2018.8604521.
7. Qu F., Qin X., Yang L., Yang T.C., (2018), Spread-spectrum method using multiple sequences for underwater acoustic communications, *IEEE Journal of Oceanic Engineering*, **43**(4): 1215–1226, doi: 10.1109/JOE.2017.2750298.
8. Ra H.-I., An J.-H., Yoon C.-H., Kim K.-M. (2021), Superimposed DSSS transmission based on cyclic shift keying in underwater acoustic communication, *OCEANS 2021 MTS/IEEE*, pp. 1–4, doi: 10.23919/OCEANS44145.2021.9706130.
9. Sarwate D.V., Pursley M.B. (1980), Cross-correlation properties of pseudorandom and related sequences, *Proceedings of the IEEE*, **68**(5): 593–619, doi: 10.1109/PROC.1980.11697.
10. Schmidt J.H. (2016), The development of an underwater telephone for digital communication purposes, *Hydroacoustics*, **19**: 341–352.

11. Schmidt J.H. (2020), Using fast frequency hopping technique to improve reliability of underwater communication system, *Applied Sciences*, **10**(3): 1172, doi: 10.3390/app10031172.

12. Schmidt J.H., Schmidt A.M. (2023) Wake-up receiver for underwater acoustic communication using in shallow water, *Sensors*, **23**(4): 2088, doi: 10.3390/s23042088.

13. Sozer E.M., Proakis J.G., Stojanovic R., Rice J.A., Benson A., Hatch M. (1999), Direct sequence spread spectrum based modem for under water acoustic communication and channel measurements, *Oceans '99. MTS/IEEE. Riding the Crest into the 21st Century. Conference and Exhibition. Conference Proceedings*, pp. 228–233, doi: 10.1109/OCEANS.1999.799743.

14. van Walree P. (2011), *Channel sounding for acoustic communications: Techniques and shallow-water examples*, FFI-Rapport 2011/00007, Forsvarets Forskningsinstitutt.

15. Zepernick H.J., Finger A. (2005), *Pseudo Random Signal Processing: Theory and Application*, John Wiley & Sons Ltd.